Chapter VII

Optical aberrations of intraocular lenses measured *in vivo* and *in vitro*

This chapter is based on the article by Barbero, et al. *Optical aberrations of intraocular lenses measured in vivo and in vitro.* J. Opt. Soc. Am. A., 2003. 20(10): p. 1841-1986.
Coauthors of the study are: Susana Marcos and Ignacio Jiménez-Alfaro
The contribution of Sergio Barbero to the study was the development, calibration and validation of the corneal aberrometry, implementation of the experimental eye model for in vitro testing of the IOLs, development of customized eye models to test computationally the optical performance of IOLs in vivo and additional computer simulations. There were also a contribution in the experimental measurements of patients, experimental data analysis and conclusions.

RESUMEN

OBJETIVOS: Medir las aberraciones totales y corneales en un grupo de ojos antes y después de la cirugía de cataratas con implantación de una lente *intraocular* (LIO) usando técnicas de aberrometría.

MÉTODOS: Las aberraciones totales se midieron con una técnica de trazado rayos. Las aberraciones corneales se obtienen a partir de una marcha de rayos partiendo de datos de elevación de un topógrafo corneal (Humphrey Instruments). Estimamos la calidad óptica de las lentes intraoculares *in vivo* restando los frentes de aberración total y corneal. Se realizaron, además, medidas de las aberraciones de las LIO *in vitro*, usando un modelo de ojo experimental, y mediante trazado de rayos virtual medimos las aberraciones de las LIO según los datos nominales dados por el fabricante.

RESULTADOS: Las aberraciones en los ojos pseudofacos no son significativamente distintas que los ojos antes de la cirugía, u ojos sin cataratas en sujetos de la misma edad; sin embargo, sí son significativamente más altas que en un grupo de ojos jóvenes. Encontramos un ligero incremento de las aberraciones corneales con la cirugía. Encontramos buena correspondencia entre las medidas de la aberración esférica *in vivo, in vitro* y simulada. A diferencia de la aberración esférica de cristalinos jóvenes, que tiende a ser negativa, la aberración esférica de la LIO es positiva, incrementado su valor con la potencia de la lente. La marcha de rayos virtual y las medidas *in vitro* muestran que desplazamientos e inclinaciones pueden contribuir al incremento de las aberraciones de tercer orden *in vivo*.

CONCLUSIONES: El efecto de la incisión, las aberraciones de la lente intraocular y la falta de compensación de la aberración esférica de la cornea por el cristalino producen degradación óptica en ojos pseudofacos.

ABSTRACT

PURPOSE: Corneal and ocular aberrations were measured in a group of eyes before and after cataract surgery with spherical intraocular lens (IOL) implantation using well-tested techniques developed in our laboratory.

METHODS: Total aberrations were measured using Laser Ray Tracing. Corneal aberrations were obtained from corneal elevation data measured with a Humphrey Instruments corneal videokeratoscope, and using custom software that performs a virtual ray tracing on the measured front corneal surface. By subtraction of corneal from total aberration maps, we estimated also the optical quality of the intraocular lens *in vivo*. We also measured the aberrations of the IOL *in vitro*, using an eye cell model, and simulated the aberrations of the IOL, based on its physical parameters.

RESULTS: We found that pseudophakic eyes do not show significantly different aberrations from eyes before cataract surgery or healthy eyes of the same age previously reported. Aberrations in pseudophakic eyes are however significantly higher than in young eyes. We found a slight increase of corneal aberrations with surgery. We found a good agreement between *in vivo*, *in vitro* and simulated measures of spherical aberration: unlike the spherical aberration of the young crystalline lens which tends to be negative, the spherical aberration of the IOL is positive and increases with lens power. Computer simulations and *in vitro* measurements show that tilts and decentrations might be contributors to the increased third order aberrations *in vivo*, in comparison to *in vitro* measurements.

CONCLUSIONS: The incision effect, the aberrations of the IOL and the lack of balance of the spherical aberration of the corneal by the spherical aberration of the intraocular lens degraded the optical quality in pseudophakic eyes.

1. Introduction

At present, surgery is the only treatment for cataract. Virtually all cataract procedures replace the natural crystalline lens by an intraocular lens (IOL). Cataract extraction and subsequent IOL implantation has evolved over the years toward less invasive procedures (smaller incisions, no sutures, etc..). The old extracapsular technique (common in the 80's) required 14-12 mm corneal incisions and multiple sutures to seal the eye after surgery, typically resulting in an astigmatism increase. Phacoemulsification was developed in the search for a way to extract cataracts through a smaller incision and it has become the preferred technique for cataract extraction. An ultrasound or laser probe is used to break the lens apart, maintaining the capsule intact. The fragments are then aspirated out of the eye. A foldable IOL is then introduced through the 3-4 mm incision. Once inside the eye, the lens unfolds to take position inside the capsule. No sutures are needed, as the incision is self-sealing. Parallel to the development of surgical procedures, new IOLs have been designed, with better optical surfaces and haptic shapes, new lens materials that minimize the loss of endothelial cells and the risk of capsule opacification, and new designs for lens positioning during surgery[1].

IOL manufacturers and researchers have developed several methods to evaluate *in vitro* IOL's optical quality. The most important are interferometric methods, Modulation Transfer Function (MTF) measurements, and resolution methods[2-4]. Efforts have been made to specify standard optical quality specifications to compare different designs and manufacturers: (American National Standard for Ophthalmics-Intraocular Lenses, and ISO 11979-2 Ophthalmics implants-Intraocular lenses-Part 2: Optical properties and test methods). Useful insight can be obtained using aberration theory[5] and with the help of optical simulations with eye models. Of particular importance are the studies by Atchison´s[6-8] and Lu et al.[9] who evaluated theoretically the impact on optical quality of different designs of IOL's. These studies predict the amount of spherical aberration associated to IOLs of different shapes.

Few studies in the literature report *in vivo* objective measurements of the optical quality of eyes implanted with IOL. Most of them measure the ocular MTF[10-12]with

double-pass techniques[13]. These studies conclude that eyes implanted with IOLs have lower MTFs (more degraded optics) than young eyes. In addition, monofocal IOLs produce better optical performance than diffractive multifocal IOLs. Double pass measurements of the MTF have proved valuable and accurate, and in addition to the contribution of aberrations, they account also for the degradation caused by scattering. However, the wave aberration produces a more complete description of optical quality, since it contains phase information and the sources of optical blur can be better discriminated.

To our knowledge, only a study by Mierdel et al[14] has measured ocular aberrations after cataract surgery and IOL implantation (using the Tscherning´s aberroscope[15]). However, the results are not very conclusive. They did not find that aberrations were significantly higher in eyes after surgery than in a group of emmetropic eyes, although higher variability in post-operative data suggested some abnormalities. Other authors have studied corneal aberration changes (due to the incision), but the results are controversial. Hayashi et al[16] found significant changes in corneal aberrations after surgery (phacoemulsification with incision length ranging from 3.5 to 6.5 mm) while Guirao et al[12] found no significant differences between post-operative corneal aberrations (extracapsular cataract extraction with 6mm incision) and corneal aberrations in an aged-matched group. Previous studies looking at corneal topography or keratometry limit their analysis to corneal astigmatism, most of them comparing the amount of post-operative corneal astigmatism with different localization[17, 18], length[19], and architecture of the incision[20]. In the present study we have combined measurements of total (using a laser ray tracing technique[21, 22]) and corneal aberrations (using a videokeratoscope and custom software[23-25]) in eyes that have undergone cataract surgery, and examined the sources of aberrations in these eyes. It is well known that optical aberrations increase with age[26, 27], mainly due to shift of spherical aberration of the crystalline lens toward positive values[28, 29]. In the present study we show that replacement of the crystalline lens by a spherical IOL does not decrease the amount of aberration in elderly eyes.

Changes in corneal aberrations allow the study of possible degradation due to the incision. Subtracting the corneal aberrations from the total aberrations provide, for the first time, measurements of the optical aberrations of the IOL *in vivo*. We also measured

the aberrations of the IOL in an optical bench, using the laser ray tracing technique and a model eye built for this purpose. Direct comparison of the aberrations of the IOL measured *in vivo* and *in vitro* allowed us to separate the optical degradation produced by the lens itself from that may be caused by positioning errors. Finally we performed optical simulations, using the proprietary designs provided to us by the manufacturer and computer eye models, in order to compare the predicted with the real optical quality.

2. Methods

A. In vivo measurements

Total wave aberrations were measured with a laser ray tracing technique, which has been described in detail in chapter II[21, 30]. Pupil dilatation was achieved using one drop of Tropicamide 1%. Pupil diameters in our old subjects ranged from 5 to 6 mm (as opposed to young subjects, for whom we typically use 6.5 mm). To facilitate comparisons across subjects, all data are presented for a 5 mm pupil diameter. Wave aberrations of the anterior corneal surface were obtained by virtual ray tracing using an optical design program (Zemax, October 17, 2002, Focus Software, Tucson, AZ). Corneal elevation maps were obtained using a videokeratographer (Humphrey Instruments, San Leandro, CA). A detailed description of the procedure, computations and validation of the technique has been presented in chapter II[23, 25, 31]. Internal aberrations were calculated by subtracting corneal aberrations from total aberrations. Internal aberrations include contributions of the crystalline lens (or IOL) and posterior corneal surface. In normal subjects posterior corneal contribution can be considered negligible[31, 32]. We quantified this contribution in 2% at most (RMS third order and higher) in an aphakic eye (chapter IV)[31].

B. In vitro measurements

The aberrations of the IOL were also measured in an optical bench using the laser ray tracing technique. The IOL was mounted following standard methods described in the literature[3, 4, 33] for MTF measurements.

For this purpose, we built an eye cell model that was mounted in place of the eye in front of the laser ray tracing technique system. Fig VII.1(a) shows a photograph of the eye cell model, and (b) a schematic diagram.

The eye cell model consisted of a 28 mm Nikkon camera objective, which acted as the cornea (RMS=0.18 μm). This lens produced the appropriate convergence onto the IOL. The IOL was placed in a container with 5-mm thick methachrylate walls, filled in with water. The IOL was mounted on a x-y linear and rotational micrometer stages, to ensure proper centration, and simulate positioning tilts. Simulations using Zemax were used to assess the appropriate distances and validity of the parameters used in this eye cell model. We computed, using the Herzberger dispersion formula[34] for 786 nm, that the error in the wave aberration measurement due to the differences in the index of refraction of water (1.3309) and those of the aqueous humor (1.3315), and the vitreous (1.3311) was negligible (0.003 μm). The distance between the camera objective and the IOL was set so that the convergence of rays on the IOL was equivalent to that of the real eye. A convergence angle of 5.1 deg (which we computed in Zemax for the post-operative cornea of eye # 7) was achieved by placing the IOL 6.08 mm behind the camera lens (and 0.8 mm from the wall of the water container).

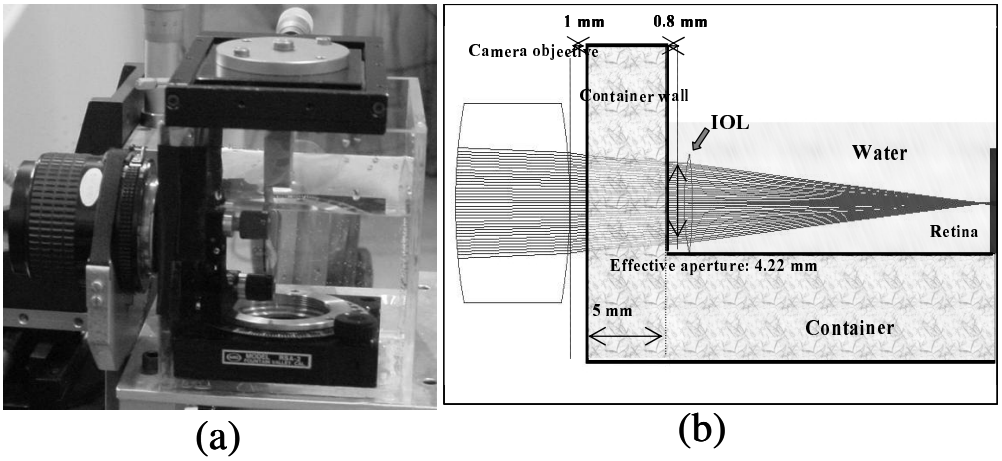

Figure VII.1: (a) Photograph of the eye cell model system used for *in vitro* measurements. **(b)** Schematic diagram of the eye cell model, consisting of a camera objective, a methachrylate cube filled with water, the IOL mounted on a rotation stage and an artificial retina.

We also computed the appropriate sampling pattern diameter to achieve a similar effective aperture of the IOL than in real eye measurements. For a distance of 4.2 mm between the posterior corneal surface and the IOL (measured by optical biometry for eye #11) and a 5-mm sampled pupil, the effective aperture on the IOL is 4.22 mm. This effective aperture was achieved by using a 5-mm pupil in the eye model. Since the measurements are done in a double-pass configuration, a diffuser surface was placed at the as focal plane, acting as the retina. In order to avoid speckle noise in the aerial images, we increased normal exposure times (100 ms) to 300 ms, while the diffuser was moved vertically. Eliminating the speckle in the images is necessary to ensure an accurate detection of the centroids. As in the real eye, we obtained sets of 37 aerial images, from which the wave aberration was computed.

To eliminate aberrations introduced by the camera lens, and especially the spherical aberration introduced container (RMS=0.09 μm), we obtained a reference set of data removing the IOL. The aberrations of the IOL (directly comparable to the internal aberrations in the eye) were computed by subtraction of this reference from the total aberrations, as the wave aberrations through different elements are additive.

C. Computer modeling

We performed computer simulations using an optical design program (Zemax) to evaluate the theoretical optical performance of the IOLs. We estimated the IOL wave aberration and spherical aberration (in terms of Z_4^0) for a model eye as function of IOL power, as well as individual predictions of total spherical aberration using individual corneal topography, anterior chamber depth and IOL parameters. This modeling also allowed us to test the effects of IOL tilt and decentration.

The computer simulations performed using monochromatic ray tracing (786 nm). Data of anterior radius, posterior radius and thickness of IOLs similar to those tested in this study were provided to us from the manufacturer, as well as refraction index (1.55). All lenses were biconvex (spherical surfaces) except for the 0 D which was a meniscus.

For comparison with *in vitro* measurement converging rays, with the same angle and the same effective pupil than in the eye cell model, were traced through the IOL. For comparison with *in vivo* measurements, we used the individual corneal elevation maps

and anterior chamber depths. The posterior corneal surface was simulated as an aspheric surface of 6.31 mm radius and -0.51 asphericity (asphericity=-e^2, where e is the conic eccentricity), these values are taken from aging corneas experimental values[35]. Corneal refraction index was assumed 1.371 (for 786 nm), and corneal thickness 0.5 mm. Estimates were obtained on the optical axis (i.e. shift of the fovea from the optical axis was not taken into account) and for the pupil centered on the optical axis.

D. Modulation Transfer Function calculations

We computed the Modulation Transfer Function (MTF), i.e. the modulus of the Optical Transfer Function (OTF), from the wave aberration using Fourier Optics and routines written in Matlab. The MTF is the modulus of the autocorrelation of the pupil function, where the pupil function is:

$$P(\alpha,\beta) = T(\alpha,\beta) * \exp(-i * \frac{2*\pi}{\lambda} * W(\alpha,\beta))$$

where W is the wave aberration and T is the pupil transmittance, α and β pupil coordinates and λ is the wavelength (786 nm). We ignored pupil apodization by Stiles-Crawford effect, i.e. $T(\alpha,\beta)=1$. MTF is calculated from the ocular wave aberrations measured *in vivo,* and from *in vitro* and simulated IOL wave aberrations. All the computations were done considering only 3rd and higher order aberrations (i.e. setting defocus and astigmatism to zero).

E. Subjects

We measured total and corneal aberrations in 9 eyes from 7 subjects (mean age: 70.6±9) after cataract surgery. Both types of measurements were conducted in the same experimental session, at least two months after surgery. Axial length and anterior chamber depth by optical biometry (IOLMaster, Humphrey-Zeiss) and autorefractometry (Automatic Refractor Model 597, Humphrey-Zeiss) were also obtained in each session. Table VII.1 provides pre- and post-operative values of the eyes under test. Some of these patients were also available before surgery. We measured total aberrations in 6 eyes of these eyes and corneal aberrations in 2 of these eyes before surgery. Post-operative corneal aberrations were also measured in an eye (# 16), not available for total aberration measurements.

All the surgeries were performed by the same surgeon using a phacoemulsification technique, with a 4.1 mm superior corneal incision (except for #16, having a 3-mm superior limbal incision) using a calibrated blade. No posterior suture was necessary. The implanted IOLs were 5.5-mm monofocal foldable lenses, with powers ranging from 0 to 26 D (mean 19.43 D). Table 1 shows the corresponding power for each subject. Four equivalent IOLs (0 D, 12 D, 16 D, and 23 D) were measured in an optical bench, with the laser ray tracing technique, as described above.

Comparisons of total and corneal aberrations were also made with respect to a group of nearly emmetropic (<4 D) and young (29±3.7) eyes, available from previous studies using the same instruments.

The study followed the tenets of the Declaration of Helsinki. Subjects were appropriately informed about the nature of the study and signed an informed consent form approved by the Institutional Ethical Committees.

PREOPERATIVE EYES

Subject	Eyes#	OD/OS	Age	Refraction	Axial Length (mm)	Anterior Chamber Depth (mm)
A	1	OS	51	-7.00 +0.25x58	25.31	2.32
B	2	OD	67	-3.25 +0.75x107	26.43	3.46
C	3	OD	81	-2.25 +1.25x3	23.42	3.09
D	4	OD	77	-1.75 +0.5x180	22.47	2.64
F	5	OS	74	+2.00 +0.75x17	22.37	3.78
F	6	OD	74	+2.00 +0.75x162	22.47	3.11

POSTOPERATIVE EYES

Subject	Eyes	OD/OS	Age	Refraction	Axial Length (mm)	Anterior Chamber Depth	IOL Power (Dp)
A	7	OD	51	-1.75 +0.00x180	30.33	4.47	0
A	8	OS	51	-3.50 +1.25x175	25.16	2.54	14
B	9	OS	67	-2.00 +1.00x13	26.07	4.94	16.5
C	10	OS	81	-1.50 +0.5x16	23.20	2.91	21
D	11	OS	77	-3.00 +3.00x18	22.46	4.2	23
E	12	OD	72	-0.25 +0.50x12	22.66	3.98	23
E	13	OS	72	-1.50 +0.5x169	22.36	4.27	23
F	14	OS	74	-1.75 +0.75x4	22.29	4.33	25.5
G	15	OD	72	-1.25 +0.25x58	22.01	3.19	26
H	16	OS	71	-2.50 +3.00x172	25.19	5.11	

Table VII.1: Refraction, axial length, anterior chamber depth and age of the eyes measured in the study. Refractive power (Dp) of the IOL implanted is also shown.

3. Results

A. In vivo measurements

Figure VII.2(a) shows post-operative total, corneal and internal wave aberration maps in all eyes measured. Tilts and defocus have been cancelled. For each eye the same gray scale has been used for all three maps, but changed across subjects. All internal wave aberration maps (excluding also astigmatism) with the same scale are represented in Figure VII.2(b). Contours are plotted at 1 μm intervals in all maps.

A great inter-eye variability is observed. In some eyes (i.e. #9, 10), the aberrations of the IOL seem to contribute more than those of the cornea to total wave aberration, while in other eyes (i.e. eye #8), the aberrations of the cornea dominate. In the rest of eyes

both, corneal, and IOL contribute significantly. Peak to valley range from □3 µm in most internal 3rd and higher other aberration patterns (see Figure VII.2(b)), indicating an important contribution of IOL aberrations *in vivo*.

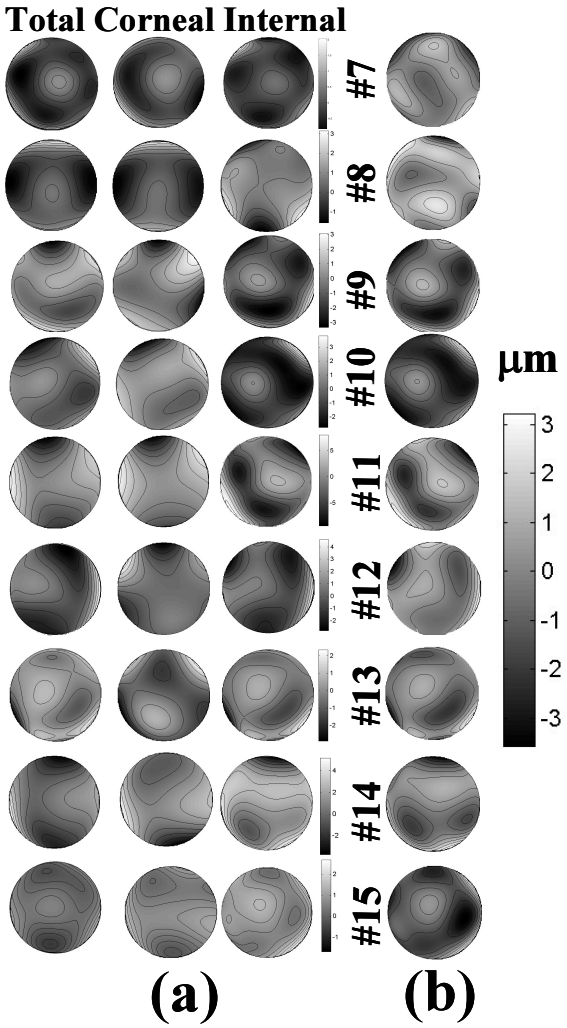

Figure VII. 2: (a) Wave aberration patterns (without tilts and defocus) of nine post-cataract surgery eyes, measured *in vivo*, for total aberrations (first column), corneal aberrations (middle column) and internal aberrations (third column). Contour lines are plotted every 1 µm. The gray scale bar represents wave aberration heights in micrometers. The same scale was used for all eyes. Diameters were 5 mm. **(b)** Internal wave aberration patterns (excluding also astigmatism) for all eyes, plotted in a common scale.

Figure VII.3 shows changes in corneal RMS, for the three eyes measured before and after surgery. 3rd & higher order aberrations increase in all 3 eyes, particularly in eye #16. Astigmatism increases in eyes # 14, 16, but not in eye# 8 that decreases from 1.18 to 0.17 D.

Figure VII.4 compares mean 3rd & higher order RMS in pseudophakic eyes with respect to the group of 6 pre-operative eyes (mean age: 70±10.55 year) and a group of 14 young nearly emmetropic eyes (mean age: 29±3.7 years).

The amount of aberrations after cataract surgery (RMS= 0.62±0.18 μm), is not significantly different (p=0.93) than in old eyes prior to cataract surgery (RMS= 0.61±0.24 μm), and it is 3.02 times higher than in young eyes. Post-operative corneal aberrations are slightly worst (RMS= 0.54±0.27 μm), but not statistically significant (p=0.24), than the pre-operative values (RMS= 0.41±0.08 μm), and significantly worst (p=0.0003) than in young eyes (RMS= 0.23±0.1 μm).

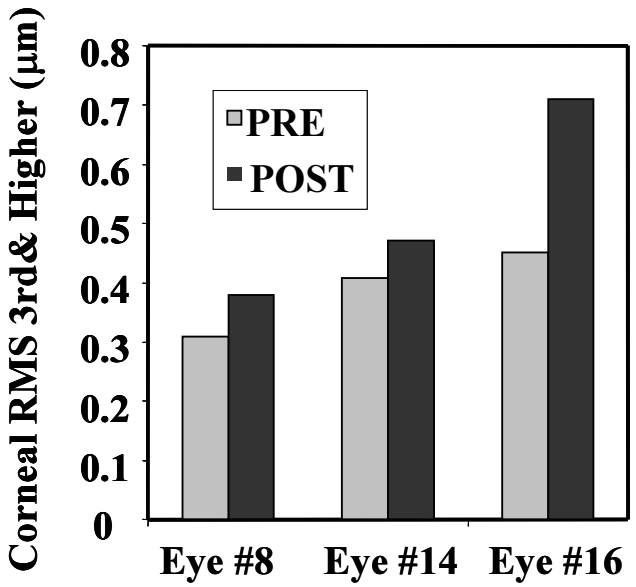

Figure VII.3: Corneal root mean square (RMS) wave aberration for 3rd and higher order aberrations, preoperative (light gray bars) and postoperative (black bars) for eyes #8, 14, and 16.

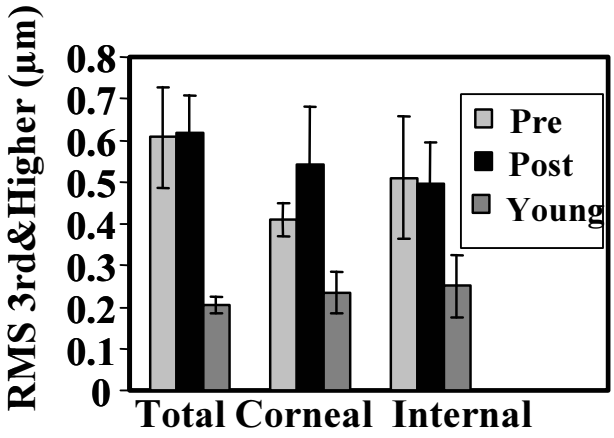

Figure VII.4: Average total, corneal and internal RMSs (3rd and higher order aberrations) for preoperative (ligth gray bars), postoperative (black bars) and young eyes (dark gray bars). Error bars stand for standard deviation.

The aberrations of our pre-operative group are similar to aberrations of healthy eyes of the same age group reported in previous studies (RMS = 0.7µm from Artal et al[36], 6 mm pupil, and RMS=1.1 µm from Mclellan et al.[26], 7.32 mm pupil, for total aberrations) and (RMS=0.5 µm from Artal et al.[36], 6 mm pupil, for corneal aberrations). Therefore this comparison could be extrapolated to a wider population.

B. *In vitro* measurements

The IOL wave aberrations of the four IOLs measured *in vitro* are shown in Figure VII.5, excluding tilts and defocus. They are all represented in the same scale.

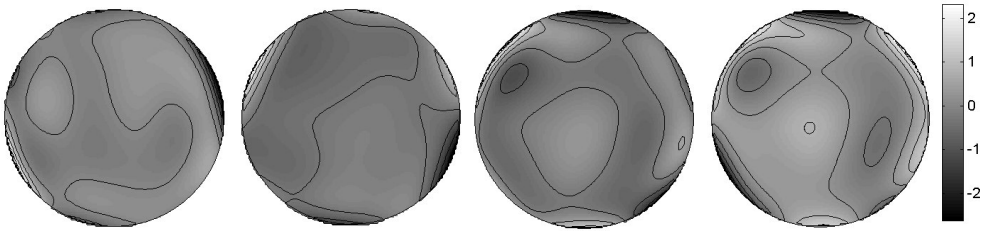

Figure VII.5: Wave aberration patterns (3th and higher order aberrations) of IOLs measured *in vitro*, using the eye cell model depicted in Fig. 1 and the laser ray tracing technique.

As for measurements *in vivo*, the amount of aberrations is significantly different from zero. The mean RMS of IOLs (excluding tilt and defocus) is 0.49±0.23 µm (as opposed to 0.47±0.3 µm for young lenses), while the RMS for 3rd and higher order aberrations is 0.34±0.01 µm, slightly larger than in young lenses (0.25±0.15 µm). This means that higher amount of astigmatism is found in natural crystalline lenses than in the IOLs measured *in vitro*, but the IOLs show higher amount of 3rd and higher order aberrations.

C. Comparison in vivo, in vitro measurements and estimations from simulations

Figure VII.6 shows comparative values of different RMS values for measurements of IOL *in vivo* and *in vitro*. Third and higher order RMS is significantly greater (2.48 times) measured *in vivo* than *in vitro* (p=0.015).

Fourth & higher RMS is not significantly different (p=0.35) between both types of measurements. The main contribution to aberrations measured *in vitro* comes from 4th and higher order aberrations, while the main contribution *in vivo* comes from 3rd order aberrations. Also, there is a larger variability *in vivo* (0.24 µm) than *in vitro* (0.09 µm) across IOL measurements.

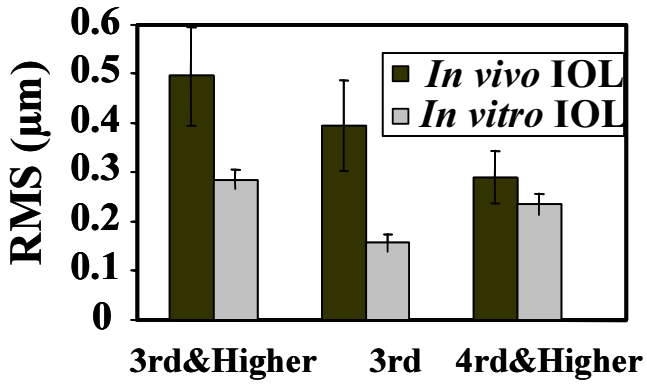

Figure VII.6: Comparison of average *in vivo* IOL (black bars) and *in vitro* IOL RMS (gray bars), for 3rd and higher order, 3rd order, 4th and higher order and astigmatism.

Figure VII.7 (a) shows the spherical aberration (Z_4^0) of the IOL from *in vivo* and *in vitro* measurements and from simulations as a function of IOL power.

There is an increase towards more positive values of spherical aberration with IOL power. The trend is similar in all type of measures indicating that the largest contribution to this effect is associated to the IOL. Except for 0 D (and one exceptional measurement *in vivo*) all values of spherical aberration are positive: 0.17±0.12 µm for *in vivo* measurements, 0.07±0.02 µm for *in vitro* measurements and 0.11±0.06 µm for simulations). The spherical aberration of the natural crystalline lens in our young group is –0.01±0.09 µm.

Simulations of IOL aberrations on-axis only produced spherical aberration, due to the symmetry of revolution of the design. Simulated tilts and decentrations of the lenses produced coma and astigmatism, and are discussed in the next section.

Figure VII.7 (b) compares total spherical aberration measured with laser ray tracing technique *in vivo* and simulations using eye models. These models include individual data of anterior corneal elevation, anterior chamber depth, and IOL design. There is a good agreement between experimental measurements and simulations from custom eye models, except for one lens (14 D).

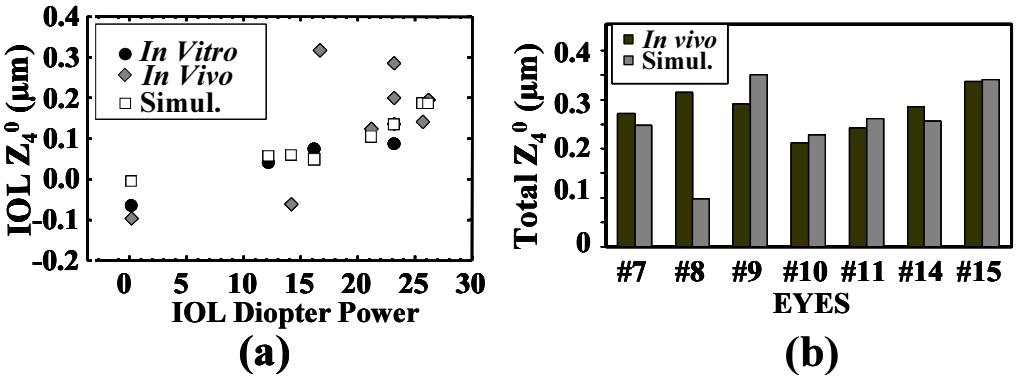

Figure VII.7: (a). Spherical aberration (Z_4^0) of the IOLs as a function of IOL power, from *in vivo* measurements (diamonds), *in vitro* measurements (circles), and from simulations (squares). **(b).** Total spherical aberration (Z_4^0), from *in vivo* experimental measurements (black bars), and simulations (gray bars) using ocular individual parameters (corneal topography, lens position, axial length) and the corresponding IOL parameters.

4. Discussion

A. Limitations of the measurements

The laser ray tracing technique proved very efficient to measure aberrations in elderly patients after surgery, and even before surgery in some patients. The fact that in this technique the aerial images are captured sequentially, and that a large area of the CCD is available for each image, allows more optical degradation (caused by aberrations or scattering) than other conventional techniques such as Shack-Hartmann. Aerial retinal images through cataracts were typically more spread and noisy than in normal eyes, due to increase in intraocular opacity and scattering[37]. In several cases the spot diagram (set of centroids computed from the aerial images) showed rather inhomogeneous patterns, probably due to large deviations of the rays produced by local lens opacities. We checked the continuity of the spot diagrams by comparing the experimental spot diagram with that derived from the computed wave aberration. Four eyes out of the 10 measured before cataract surgery were excluded because the lack of correspondence of computed and simulated spot diagrams. Aerial retinal images from post-operative eyes typically showed larger halos than in normal eyes. This is probably due to higher reflectivity of the IOL surfaces[38], caused by their higher index of refraction (1.55, *versus* less than 1.395[39] in the natural lens). Centration and stability of subjects head during measurement was also typically poorer in elderly patients than in normal young subjects. As a result of the above, the measurement variability was slightly larger in these measurements, than in previous studies in young subjects. Zernike coefficient standard deviation (averaged across terms) was 0.1±0.03 µm and 0.18±0.19 µm pre- and post-operative respectively, while for the young reference group the standard deviation was 0.05±0.02 µm.

B. Sources of aberrations after cataract surgery

1. Corneal aberrations.

Our analysis of pre- and post-operative corneal aberrations is limited to three eyes, and therefore does not have sufficient statistical power. However, all three corneas show an increase in 3rd and higher order RMS: 0.07, 0.06 and 0.26 µm in eyes #8, 14, 16 respectively. It has been reported that, although to a much lesser extent than in previous

techniques requiring a suture, the small incision in phacoemulsification induces slight changes in astigmatism. Our results suggest that higher order aberrations are also modified and tend to increase (Figure VII.3). The incision was performed in the vertical meridian, and superior in all eyes of this study. Incision on the steepest meridian has been reported to produce a relaxation of this meridian, therefore avoiding post-operative astigmatism, for pre-operative astigmatism of 0.5 D or higher[40]. Pre-operative corneal astigmatic axis was against the rule (2.3º and 172.1º) in eyes # 14,16 respectively. In these eyes the incision is produced in the flattest meridian, instead of the steepest, which results in an increase of astigmatism. Pre-operative astigmatism was with the rule (88.6º) in eye#8, and as expected, astigmatism decreases after surgery.

2. Aberrations of the IOL.

Measurements *in vivo* and *in vitro* show that positive spherical aberration is present in IOLs. The spherical aberration increases with the IOL power. Comparison with computer simulations show that the spherical design of the IOL surfaces results in the observed positive spherical aberration. These results agree with previous predictions by Atchison et al[7]. Fifth and higher order terms are present in both *in vivo* and *in vitro* measurements, but not in results from computer simulations (based on IOLs with purely spherical surfaces).

3.IOL's Tilt and decentration

Except for the spherical aberration , the *in vivo* IOL aberrations are higher in most terms (particularly 3rd order aberrations) than the equivalent measures *in vitro*.

There are several studies in the literature reporting tilts and decentrations of different types of pseudophakic IOLs, based on measurements using Purkinje images or Scheimpflug lamp biomicroscopy. Using Purkinje images, Philips et al[38] reported average tilt values of 7.8 deg and 0.7 mm in decentration[38]. Mutlu et al[41] reported lower values: mean tilt of 2.83 deg and mean decentration of 0.28 mm. Jung et al.[42] reported tilts of up to 3.01 deg (mean tilts of 2.35 deg) measured using a Scheimpflug lamp.

Our study has not directly measured the tilts and decentration of IOLs *in vivo*. Using the eye cell model and computer simulations, we evaluated the effect of plausible IOL tilts and decentrations on the aberration pattern. Figure VII.8 (a) shows results of RMS

(for 3rd and higher order aberrations) for an IOL of 16 D, for centered, and tilted positions of 4 and –4 deg respectively. Tilts were achieved by physically rotating the lens using a micrometer stage within the cell, or computationally rotating the lens around the horizontal axis.

Third order RMS increase on average by 0.15 µm with respect to the centered position for a tilt of 4 deg, comparable to results from the simulations (0.10 mm) (see Figure VII.8 (a). Results from simulations show that 3rd order RMS increases linearly with IOL decentration, by 0.045 µm for 0.5-mm decentration. (Figure VII.8 (b)). Combined tilt and decentration are most likely present in real eyes. No particular trend has been reported in the literature for the direction of decentration[38, 43]. Tilts seem more predominant along the horizontal or vertical axis[38]. We tested the effect of various tilts, for a certain amount of decentration (0.5 mm), Fig. 8 c, the effects of various amounts of decentrations for a given tilt, Figure VII.8 d). Our simulations show that some specific combinations of tilt and decentration may counteract the induction of 3rd order aberrations, while other combinations add up the effect (Figure VII.8 b) and c)), indicating that the correlation between tilts/decentrations and 3rd order aberrations present in real eyes implanted with IOLs can be complex. Experimental measurements of tilts and decentrations in each individual eye are necessary to quantify their actual impact on 3rd order aberrations measured in each eye.

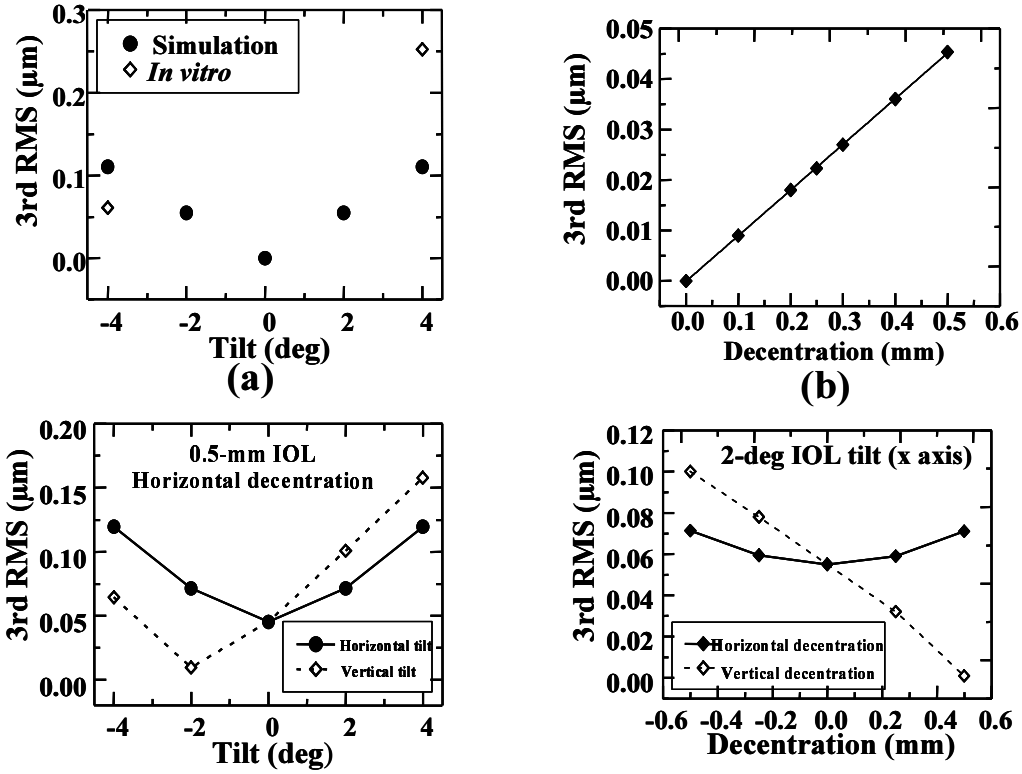

Figure VII.8: (a). Changes in IOL RMS (3rd order) as a function of tilt from *in vitro* measurements (empty diamonds) and from simulations (filled circles). **(b).** Simulated IOL 3rd order RMS as a function of lens decentration. **(c).** Simulated IOL's 3rd order RMS as a function of lens horizontal and vertical tilts, for or a fixed simulated 0.5 mm IOL horizontal decentration **(d).** Simulated IOL's 3rd order RMS as a function of horizontal and vertical decentrations of the IOL, for a fixed simulated 2 deg IOL tilt (horizontal axis).

4. Lack of balance corneal/internal aberrations.

This increase of the total aberrations with age in our study is in agreement with some works reported previously in the literature[26]. This can be due to two factors: 1) The increase of corneal and lenticular aberrations. The old/young RMS ratio is 2.04 for internal aberrations and 1.75 for corneal aberrations; 2) A certain degree of loss of balance between corneal and internal aberrations (as found by Artal et al[36]). Total RMS in young eyes is lower that corneal RMS, while in old eyes total RMS is 1.48 higher than corneal RMS.

It seems widely accepted that the natural crystalline lens corrects to some extent the aberrations of the cornea, particularly the spherical aberration. Artal et al.[12, 36] suggested that this balance was disrupted with aging. A reasonable explanation is that with aging, the spherical aberration of the crystalline lens shifts toward more positive values, as

reported by *in vivo*[29] and *in vitro* studies[44]. Our data show that the spherical aberration of the IOL is positive, as opposed to negative in young eyes (Figure VII.7(a) and Figure VII.9). It is then expected that, as found in old natural eyes, a lack of balance between corneal and internal spherical aberration is also responsible for the increased RMS in pseudophakic eyes with respect to young eyes.

Using RMS ratios is not an optimal way to evaluate the degree of corneal-to-internal balance, because the RMS does not take into account the coefficient sign and multiple cross-terms prevent from a direct analysis. Instead, we performed a term by term analysis and evaluated, for each term, the amount of corneal correction by the crystalline lens and *viceversa.* For each eye, we defined a series of 37 compensation values (corresponding to the 37 Zernike coefficients). Compensation values (*CVi*) were defined as $CVi=\text{sign}(C_{corneai}/C_{internali})*\min(C_{corneai},C_{internali})$. The rationale for this definition is as follows: The first term (sign of cornea/internal ratio) indicates presence (if negative) or absence (if positive) of compensation. If both corneal and internal coefficients have different sign, then some compensation occurs, while if they both have the same sign (positive term) they will add up. The second term is indicative of the amount of compensation. The minimum value between $C_{corneai}$ and $C_{internali}$ represents the amount of aberration subtracted from the aberration of the dominant component (if sign is different for $C_{corneai}$ and $C_{internali}$) or the amount that adds up (if both have the same sign for $C_{corneai}$ and $C_{internali}$). Therefore, a high term value with a negative sign is indicative of a high degree of compensation between ocular components, while a high term with a positive value is indicative of an addition of the aberrations. We found a slight loss of balance of 3rd order terms with age (average *CVi* -0.079 for young, and -0.049 µm for old eyes, respectively) but no significant difference with between young and post-operative eyes (–0.087 µm). Compensation values for astigmatism and spherical aberration show important differences. Average *CVi* for astigmatism is -0.178 µm in young eyes, on average, while for old and post-operative eyes it shows positive values (0.040 and 0.045 µm, respectively) indicating a lack of compensation. For spherical aberration, we found negative values for young eyes (–0.025 µm), indicating compensation, and positive values in old and post-operative eyes (0.007 and 0.03 µm, respectively). Figure VII.9 shows total, corneal and internal spherical values (Z_4^0) for young, pre-operative and post-operative eyes.

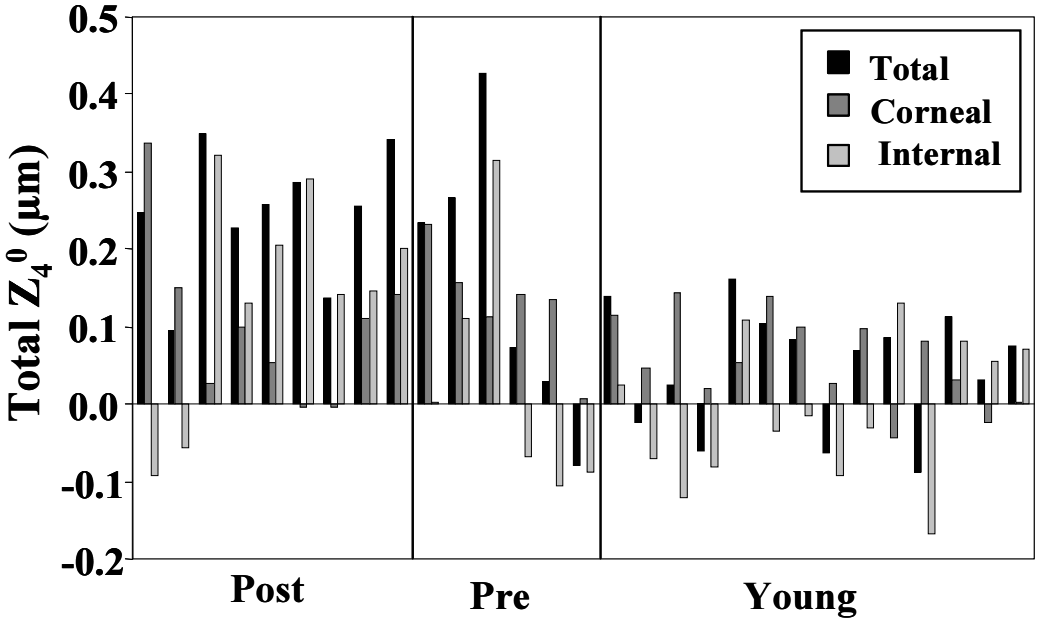

Figure VII.9: Total (black bars), corneal (dark grey bars) and internal (light grey bars) spherical aberration (Z_4^0) for young, pre-operative and post-operative eyes.

C. Modulation Transfer Functions: *in vivo* and *in vitro* measurements

All previous *in vivo* data of optical quality after cataract surgery were obtained using a double-pass technique[10-12], which can only provide the MTF. Most *in vitro* assessments of the optical quality of IOLs are based on MTF measurements[2-4]. We computed MTFs from the measured wave aberrations *in vivo* (total and IOL MTF), and *in vitro* and simulated wave aberrations (IOL MTF).

In Figure VII.10 we compare total average MTF of the group of young and post-operative eyes, with previous *in vivo* data reported in literature using double-pass techniques.

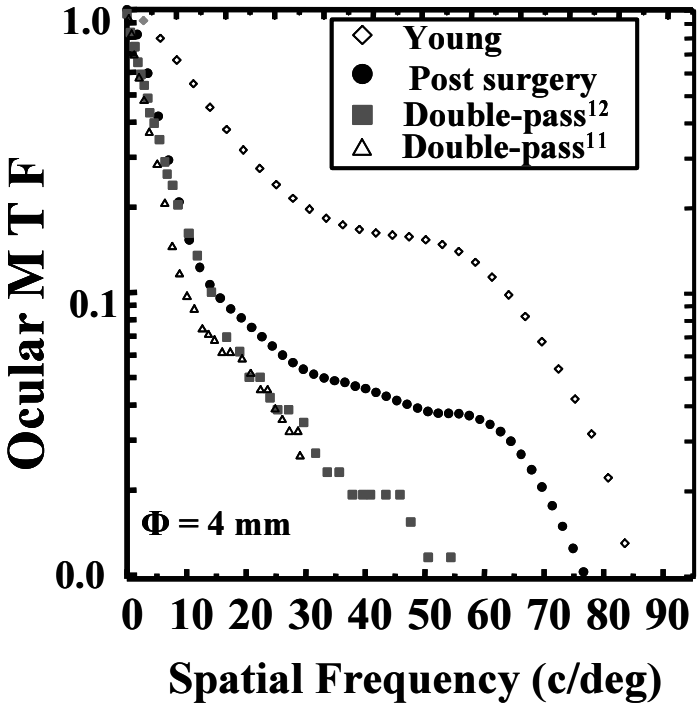

Figure VII.10: Average MTF (radial profile), computed from the wave aberrations, for the young and postoperative group in comparison to double-pass MTF measurements from previous studies by Artal et al (1995) and Guirao et al (2002). Pupil diameter= 4 mm.

These previous studies measured a group of patients implanted with monofocal PMMA IOLs after extracapsular cataract extraction[12], and a group with monofocal IOLs (FORMFLEX II, IOLAB)[11], respectively. The MTF is substantially higher for young eyes than any post-operative measurement, for the entire spatial frequency range. Differences between post-operative data from our study and other groups' are smaller than with respect to data in young eyes, despite the different surgical techniques and IOLs. However, our *in vivo* MTFs are significantly higher, particularly for high frequencies, than those measured previously. The fact that the surgical technique is less invasive (minimizing the impact of the incision) and possible differences across the different type of lenses can be potential reasons for the improvement. In addition double-pass MTFs have been found to be consistently lower than MTFs estimated from wave aberrations, because they are affected by scattering and higher order aberrations non measured by aberrometers. This may be also a cause for the discrepancy. The potential influence of retinal scattering in double-pass measurements in older eyes has

never been studied, and therefore we cannot quantify its relative contribution to the difference.

Figure VII.11 shows the MTFs due only to internal aberrations. The optical quality of young lenses appears to be clearly better than IOLs for all frequencies.

Figure 12 compares MTFs of the IOL from *in vitro* measurements with previous *in vitro* measurements on acrylic IOLs[45]and polymethyl methacrylate (PMMA) IOLs[4]. MTFs from computer ray tracing simulations on the IOLs from our study are also included. For a proper comparison with earlier works, we recalculated the MTF for 3-mm diameter aperture. Comparing our *in vivo* measurements with those of Oshika et al[45] and Norrby et al[4] we found no significant differences except for the higher spatial frequencies beyond 35 c/deg. The MTF predicted from the optical design of the IOLs of this study is significantly higher than other measurements (except for frequencies beyond 40 c/deg, where PMMA *in vitro* measurements show slightly higher values). The fact that there is a consistent discrepancy between predictions and measurements on the optical bench may be indicative of some differences between theoretical designs and final lens manufacturing and experimental handling.

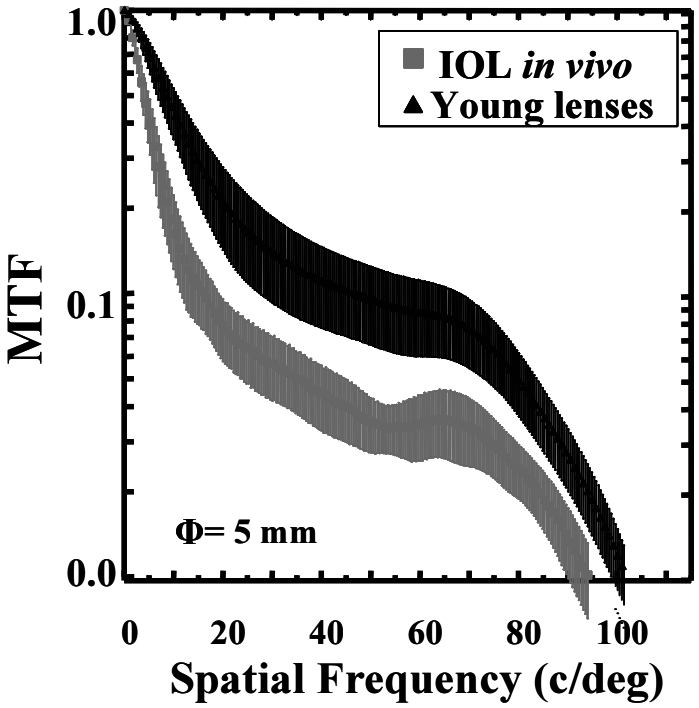

Figure VII.11: Average MTF (radial profile), computed from the wave aberration, for a group of young crystalline lenses and IOLs, both measured *in vivo*. Pupil diameter= 5 mm. Error bars stand for standard deviation across eyes.

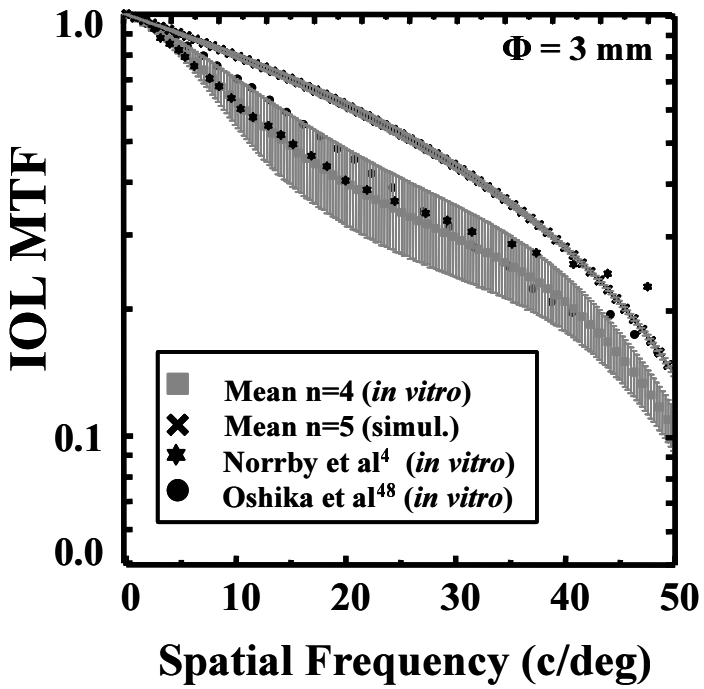

Figure VII.12: Average MTF (radial profile), computed from the wave aberration, for *in vitro* measurements and simulations from this study, and *in vitro* MTF measurements by Oshika et al (1996) and Norrby et al (1998). Pupil diameter= 3 mm. Error bars stand for standard deviation of the in vitro measurements across eyes.

5. Conclusions

1. We have measured, for the first time, the aberrations of IOLs *in vivo*.

2. Previous *in vivo* data were limited to MTFs, measured by double pass techniques. The use of corneal and total wave aberrations allowed us to estimate the sources of degradation of optical quality in eyes after cataract surgery.

3. Optical quality after cataract surgery is significantly lower in pseudophakic eyes (RMS for 3rd and higher order terms 0.62±0.18 μm) than in young eyes (0.2±0.04 μm). The amount of aberrations in pseudophakic eyes is similar to phakic eyes of the same age group. These conclusions are based on a small data set, but show a very consistent trend are highly statistically significant.

4. From measurements of spherical IOLs *in vivo*, *in vitro* and computer simulations we conclude that the spherical aberration of the IOL (which is positive, and increases

with IOL power) is a source of optical degradation. As opposed to young eyes, there is no balance of corneal and internal spherical aberrations and atigmatism.

5. IOL's 3rd order aberrations measured *in vivo* are much higher (0.4±0.18 μm) than *in vitro* (0.16±0.04 μm). IOL tilts and decentrations could be responsible for this further decrease in optical quality.

6. IOL optical quality (measured both *in vivo* and *in vitro)* is lower than predicted from simulations, possibly indicating some discrepancies from the theoretical design.

7. Laser Ray Tracing and Corneal Topography are useful techniques to understand the optical changes induced by cataract surgery. These measurements allow to validate predictions of optical quality with IOLs using individual eye models, and to explore possible new designs.

6. References

1. D. T. Azar, *Intraocular lenses in cataract and refractive surgery* (W.B. Saunders Company, Philadelphia, 2001).
2. M. J. Simpson, "Optical quality of intraocular lenses," J Cataract Refract surg 18, 86-94 (1992).
3. V. Portney, "Optical testing and inspection methodology for modern intraocular lenses," J Cataract Refract Surg 18, 607-613 (1992).
4. N. E. Norrby, L. W. Grossman, E. P. Geraghty, C. F. Kreiner, M. Mihori, A. S. Patel, V. Portney, and D. M. Silberman, "Determining the imaging quality of intraocular lenses," J Cataract Refract Surg 24, 703-714 (1998).
5. G. Smith and C. W. Lu, "The spherical aberration of intraocular lenses," Ophthal Physiol Opt 8(3), 287-294 (1988).
6. D. Atchison, "Third-order aberrations of pseudophakic eyes," Ophthal Physiol 9, 205-210 (1989).
7. D. A. Atchison, "Optical design of intraocular lenses. I. On-axis performance," Optom Vis Sci 66, 492-506 (1989).
8. D. Atchison, "Design of aspheric intraocular lenses," Ophthalmic Physiol Opt 11(2), 137-146 (1991).
9. C. W. Lu and G. Smith, "Aspherizing of intra-ocular lenses," Ophthal Physiol Opt 10(1), 54-66 (1990).
10. R. Navarro, M. Ferro, P. Artal, and I. Miranda, "Modulation transfer functions of eyes implanted with intraocular lenses," App Opt 32, 6359-6367 (1993).
11. P. Artal, S. Marcos, R. Navarro, I. Miranda, and M. Ferro, "Through focus image quality of eyes implanted with monofocal and multifocal intraocular lenses," Optical Engineering 34, 772-779 (1995).
12. A. Guirao, M. Redondo, E. Geraghty, P. Piers, S. Norrby, and P. Artal, "Corneal optical aberrations and retinal image quality in patients in whom monofocal intraocular lenses were implanted," Archives of Ophthalmology 120, 1143-1151 (2002).
13. J. Santamaria, P. Artal, and J. Bescós, "Determination of the point-spread function of human eyes using a hybrid optical-digital method," J. Opt. Soc. Am. - A 4, 1109-1114 (1987).
14. P. Mierdel, M. Kaemmerer, H. E. Krinke, and T. Seiler, "Effects of photorefractive keratectomy and cataract surgery on ocular optical erros of higher order," Graefe´s Arch Clin Exp Ophthalmol 237, 725-729 (1999).

15. M. Mrochen, M. Kaemmerer, P. Mierdel, H. E. Krinke, and T. Seiler, "Principles of Tscherning Aberrometry," J Refract Surgery 16, S570-S571 (2000).
16. K. Hayashi, H. Hayashi, T. Oshika, and F. Hayashi, "Fourier analysis of irregular astigmatism after implantation of 3 types of intraocular lenses," J Cataract Refract Surg 26, 1510-1516 (2000).
17. T. Oshika, G. Sugita, T. Tanabe, A. Tomidokoro, and S. Amano, "Regular and irregular astigmatism after superior versus temporal scleral incision cataract surgery," Ophthalmology 107, 2049-2053 (2000).
18. R. Gross, "Corneal astigmatism after phacoemulsification and lens implantation through unsutured scleral and corneal tunnel incisions," Am J Ophthalmol 121, 57-64 (1996).
19. T. Kohnen, B. Dick, and K. Jacobi, "Comparison of the induced astigmatism after temporal clear corneal tunnel incisions of different sizes," J Cataract Refract Surg 21(4), 417-424 (1995).
20. P. Nielsen, "Prospective evaluation of surgically induced astigmatism and astigmatic keratotomy effects of various self-sealing small incisions," J Cataract Refract Surg 21, 43-48 (1995).
21. R. Navarro and M. A. Losada, "Aberrations and relative efficiency of light pencils in the living human eye," Optom Vis Sci 74, 540-547 (1997).
22. R. Navarro and E. Moreno-Barriuso, "Laser ray-tracing method for optical testing," Optics Letters 24(14), 1-3 (1999).
23. S. Barbero, S. Marcos, J. Merayo-Lloves, and E. Moreno-Barriuso, "A validation of the estimation of corneal aberrations from videokeratography: test on keratoconus eyes," J Refract Surg 18, 267-270 (2002).
24. C. Dorronsoro, S. Barbero, L. Llorente, and S. Marcos, "Detailed on-eye measurement of optical performance of rigid gas permeable contact lenses based on ocular and corneal aberrometry," Opt Vis Sci 80(2), 115-125 (2003).
25. S. Marcos, S. Barbero, L. Llorente, and J. Merayo-Lloves, "Optical Response to Myopic LASIK Surgery from Total and Corneal Aberration Measurements," Invest Ophthalmol Vis Sci 42, 3349-3356 (2001).
26. J. McLellan, S. Marcos, and S. A. Burns, "Age-related changes in monochromatic wave aberrations of the human eye," Invest Ophthalmol Vis Sci 42, 1390-1395 (2001).
27. A. Guirao, M. Redondo, and P. Artal, "Optical aberrations of the human cornea as a function of age," J Opt Soc Am A 17, 1697-1702 (2000).
28. A. Glasser and M. Campbell, "Presbyopia and the optical changes in the human crystalline lens with age," Vision Research 38(2), 209-229 (1998).
29. G. Smith, M. J. Cox, R. Calver, and L. F. Garner, "The spherical aberration of the crystalline lens of the human eye," Vision Res 41, 235-243 (2001).
30. E. Moreno-Barriuso, S. Marcos, R. Navarro, and S. Burns, "Comparing Laser Ray Tracing, Spatially Resolved Refractometer and Hartmann-Shack Sensor to measure the ocular wave aberration," Optom Vis Sci 78, 152-156 (2001).
31. S. Barbero, S. Marcos, and J. Merayo-Lloves, "Exploring total and corneal aberrations in an unilateral aphakic subject," J Cataract Refract Surg 28(9), 1594 (2002).
32. A. Guirao and P. Artal, "Corneal wave aberration from videokeratography: accuracy and limitations of the procedure," J Opt Soc Am A 17, 955-965 (2000).
33. M. J. Simpson, "Diffractive multifocal intraocular lens image quality," Applied Optics 31(19), 3621-3626 (1992).
34. M. Herzberger, "Colour Correction in Optical Systems and a New Dispersion Formula," Optica Acta 6, 197-215 (1959).
35. M. Dubbelman, H. A. Weeber, R. G. Van der Heijde, and H. J. Volker-Dieben, "Radius and asphericity of the posterior corneal surface determined by corrected Scheimpflug photography," Acta Ophthalmol Scand 80(4), 379-383 (2002).
36. P. Artal, E. Berrio, A. Guirao, and P. Piers, "Contribution of the cornea and internal surfaces to the change of ocular aberrations with age," J Opt Soc Am A 19, 137-143 (2002).
37. P. Waard, J. Jspeert, T. Van de Berg, and P. Jong, "Intraocular ligth scattering in age-related cataracts," Invest Ophthalmol Vis Sci 33, 618-625 (1992).
38. P. Philips, H. Rosskothen, J. Emmanuelli, and C. Koester, "Measurement of intraocular lens decentration and tilt in vivo," J Cataract Refract Surg 14, 129-135 (1988).
39. G. Smith and B. K. Pierscionek, "The optical structure of the lens and its contribution to the refractive status of the eye," Ophthal Physiol Opt 18, 21-29 (1997).

40. Y. Matsumoto, T. Hara, K. Chiba, and M. Chikuda, "Optimal incision sites to obtain an astigmatism-free cornea after cataract surgery with a 3.2 mm sutureless incision," J Cataract Refract Surg 27, 1615-1619 (2001).
41. F. Mutlu, A. Bilge, H. Altinsoy, and E. Yumusak, "The role of capsulotomy and intraocular lens type on tilt and decentration of polymethylmethacrylate and foldable acrylic lenses," Ophtalmologica 212(6), 359-363 (1998).
42. C. K. Jung, S. K. Chung, and N. H. Baek, "Decentration and tilt: Silicone multifocal versus acrylic soft intraocular lenses," J Cataract Refract Surg 26, 582-585 (2000).
43. M. Wang, L. Woung, C. Hu, and H. Kuo, "Position of poly(methyl methacrylate) and silicone intraocular lenses after phacoemulsification," J Cataract Refract Surg 24, 1652-1657 (1998).
44. A. Glasser and M. Campbell, "Biometric, optical and physical changes in the isolated human crystalline lens with age in relation to presbyopia," Vis. Res. 39, 1991-2015 (1999).
45. T. Oshika and Y. Shiokawa, "Effect of folding on the optical quality of soft acrylic intraocular lenses," J Cataract Refract Surg 22, 1360-1364 (1996).